Gills are an initial target of zinc oxide nanoparticles in oysters Crassostrea gigas, leading to mitochondrial disruption and oxidative stress

Rafael Trevisan, Gabriel Delapedra, Danielle Mello, Miriam Arl, Éder Schmidt, Fabian Meder, Marco Monopoli, Eduardo Cargnin-Ferreira, Zenilda Bouzon, Andrew Fisher, et al.

GILLS ARE AN INITIAL TARGET OF ZINC OXIDE NANOPARTICLES IN OYSTERS *CRASSOSTREA GIGAS*, LEADING TO MITOCHONDRIAL DISRUPTION AND OXIDATIVE STRESS.

Rafael Trevisan[1], Gabriel Delapedra[1], Danielle F. Mello[1], Miriam Arl[1], Éder C. Schmidt[2], Fabian Meder[3], Marco Monopoli[3], Eduardo Cargnin-Ferreira[4], Zenilda L. Bouzon[2], Andrew S. Fisher[5], David Sheehan[6], Alcir L. Dafre[1,*]

[1] Department of Biochemistry, Federal University of Santa Catarina, 88040-900 Florianópolis, SC, Brazil

[2] Department of Cell Biology, Embryology and Genetic, Federal University of Santa Catarina, 88049-900, Florianópolis, SC, Brazil

[3] Centre for Bionano Interactions, University College Dublin, Dublin, Ireland

[4] Federal Institute of Santa Catarina, Campus Garopaba, Laboratory of Histological Markers, 88495-000 Garopaba, SC, Brazil

[5] School of Geography, Earth and Environmental Sciences, University of Plymouth, PL4 8AA Plymouth, United Kingdom

[6] Department of Biochemistry, University College Cork, Cork, Ireland.

*Corresponding author: Alcir L. Dafre, Department of Biochemistry, Biological Sciences Centre, Federal University of Santa Catarina, 88040-900 Florianópolis, SC, Brazil
Fax. +55 48 3721-2827
Email: alcir.dafre@ufsc.br

HIGHLIGHTS

ZnONP exposure causes an initial accumulation of zinc in gills and later in digestive gland.

Zinc burden occurs by ZnONP endocytosis or uptake of ionic zinc after dissociation.

ZnONP exposure disrupts mitochondrial ultrastructure in both tissues.

Mitochondrial damage and oxidative stress are major features of ZnONP acute toxicity.

ABSTRACT

The increasing industrial use of nanomaterials during the last decades poses a potential threat to the environment and in particular to organisms living in the aquatic environment. In the present study, the toxicity of zinc oxide nanoparticles (ZnONP) was investigated in Pacific oysters *Crassostrea gigas*. The nanoscale of ZnONP, in vehicle or ultrapure water, was confirmed, presenting an average size ranging from 28 to 88 nm. In seawater, aggregation was detected by TEM and DLS analysis, with an increased average size ranging from 1 to 2 µm. Soluble or nanoparticulated zinc presented similar toxicity, displaying a LC_{50} (96 h) around 30 mg/L. High zinc dissociation from ZnONP, releasing ionic zinc in seawater, is a potential route for zinc assimilation and ZnONP toxicity. To investigate mechanisms of toxicity, oysters were treated with 4 mg/L ZnONP for 6, 24 or 48 h. ZnONP accumulated in gills (24 and 48 h) and digestive glands (48 h). Ultrastructural analysis of gills revealed electron-dense vesicles near the cell membrane and loss of mitochondrial cristae (6 h). Swollen mitochondria and a more conspicuous loss of mitochondrial cristae were observed after 24 h. Mitochondria with disrupted membranes and an increased number of cytosolic vesicles displaying electron-dense material were observed 48 h post exposure. Digestive gland showed similar changes, but these were delayed relative to gills. ZnONP exposure did not greatly affect thiol homeostasis (reduced and oxidized glutathione) or immunological parameters (phagocytosis, hemocyte viability and activation and total hemocyte count). At 24 h post exposure, decreased (–29%) glutathione reductase (GR) activity was observed in gills, but other biochemical responses were observed only after 48 h of exposure: lower GR activity (–28%) and levels of protein thiols (–21%), increased index of lipid peroxidation (+49%) and GPx activity (+26%). In accordance with ultrastructural changes and zinc load, digestive gland showed delayed biochemical responses. Except for a decreased GR activity (–47%) at 48 h post exposure, the biochemical alterations seen in gills were not present in digestive gland. The results indicate that gills are able to incorporate zinc prior (24 h) to digestive gland (48 h), leading to earlier mitochondrial disruption and oxidative stress. Our data suggest that gills are the initial target of ZnONP and that mitochondria are organelles particularly susceptible to ZnONP in *C. gigas*.

Keywords: nanomaterials; bivalves; antioxidants; glutathione reductase; mitochondria

1. Introduction

In recent years, the synthesis and manufacturing of nanomaterials has greatly increased due to interest on their unique physical and chemical properties (Nel et al., 2006). The relatively small size of these compounds, ranging from 1 to 100 nm and with a greatly increased surface area/volume ratio,

confers specific characteristics that are not usually found in their bulk counterparts. These properties allow their application in several economic areas with an estimated market of $ 1 trillion by 2015 (Nel et al., 2006). In parallel to this potential of nanotechnology, awareness about the effects of such compounds to human health and to the environment has also increased, originating a new research area named nanotoxicology. It is essential to understand and characterize the adverse effects of nanomaterials to permit formulation of adequate policies and, consequently, safer use of nanomaterials (Hristozov et al., 2012).

The toxicity of nanomaterials has been addressed *in vivo* or *in* vitro in different models, revealing effects such as: production of reactive oxygen species (ROS), induction of oxidative stress, macromolecular damage, cellular and organelle disturbances, and cell death (Arora et al., 2012; Nel et al., 2006). Although many nanotoxicological studies are related to the effects on human health, research has also been conducted with non-mammalian organisms, especially with aquatic species. Aquatic ecosystems are considered a final destination for many chemicals, including nanomaterials, but information about the fate of nanomaterials in such environments is still scarce (Scown et al., 2010). In addition, relatively little is known about the processes of absorption, metabolism and excretion of nanomaterials by aquatic organisms (Handy et al., 2008). Toxicological studies are crucial to increasing our knowledge about the fate and effects of nanomaterials in aquatic environments and organisms.

In this study, we focused on the effects of zinc oxide nanoparticles (ZnONP). These have unique optical and electrical properties and are components of many commercial products, including: personal care products, plastics, ceramics, glass, cement, rubber, lubricants, paints, pigments, food, batteries and fire retardants (Ma et al., 2013). The toxicity of ZnONP, just like other metal oxide nanoparticles, is related to the ionic dissociation (Zn^{2+}) in water, generation of ROS through media-surface interactions and interaction with biological targets, for instance destabilization of lipid membranes and damage to proteins and DNA (Ma et al., 2013).

Bivalves have been considered a target group for nanoparticle toxicity for two main reasons: (i) endocytosis and phagocytosis processes in digestive-related organs such as the digestive gland, in epithelial limits such as mantle and gills and in immunological cells such as hemocytes; (ii) a filter-feeding habit that is characterized for large volumes of filtered water (Canesi et al., 2012; Moore, 2006). Research data also confirm this proposition: silver nanoparticles are toxic to the development of oyster embryos (Ringwood et al., 2010) and to shell calcification in mussels (Zuykov et al., 2011); copper nanoparticles induce oxidative processes in mussels (Gomes et al., 2011, 2012) and behavioral disturbances in clams (Buffet et al., 2011); gold nanoparticles caused oxidative damage and lysosomal instability in mussels (Tedesco et al., 2010a, 2010b). However, little is known about ZnONP toxicity to bivalves.

In the present study, we investigated the effects of ZnONP to the Pacific oyster *Crassostrea gigas* during acute exposure. The determination of the LC_{50} (96 h) was initially carried out to understand more about the toxicity of ZnONP to this species. In addition, accumulation of zinc in gills and digestive gland after 24 and 48 h was assessed. Ultrastructural and biochemical analysis in gills and digestive gland indicates significant toxicity potential of ZnONP.

2. Materials and Methods

2.1. ZnONP characterization

ZnONP were purchased as dispersion in butyl acetate (Sigma Aldrich #721093, São Paulo, Brazil). Characterization of the nanoparticles was carried by transmission electron microscopy (TEM) and dynamic light scattering (DLS).

For TEM analysis, ZnONP dispersion was first diluted in dimethyl sulfoxide (DMSO) followed by dilution in seawater, to a final concentration of 50 mg/L ZnONP. An aliquot was allowed to air dry on a copper grid and analyzed at 80 KV by a JEM-1011 (JEOL, Japan) electron microscope. The primary nanoparticle size was determined from images of 1000 randomly selected nanoparticles using the Image J software for quantification (version 1.47; downloaded from http://rsb.info.nih.gov/ij/).

For DLS analysis, ZnONP solutions were prepared in pure DMSO or in seawater, ranging from 8 to 32 mg/L. The samples were analyzed in a Zetasizer Nano series (Malvern Instruments, UK). Two replicates were analyzed for each sample, with 11 readings per replicate. DMSO was used as solvent carrier to characterize the nanoparticles dispersion because it was also used to pre-dilute the nanoparticles prior the animal exposure protocols.

2.2. Animals and exposure conditions

Adult male and female Pacific oysters *C. gigas* (10.7 ± 0.81 cm and 70.6 ± 10.34 g) were obtained from an aquaculture farm at Florianópolis, Brazil. Prior to experiments, animals were maintained for 7 days in plastic aquaria with 1 L of filtered and sterilized seawater per animal, with a natural daylight cycle and temperature ranging from 18-20 ˚C. Animals were fed with commercial phytoplankton-based food every two days.

An initial experiment was carried out to estimate the ZnONP LC_{50} (96 h) to *C. gigas*: animals were exposed to ZnONP at nominal concentrations from 50 µg/L to 50 mg/L (1 L seawater/animal, 2 tanks of 7 animals per group) for 96 h, with daily water change and ZnONP renewal. Zinc chloride ($ZnCl_2$) acute toxicity was also similarly assessed in *C. gigas* in order to evaluate the toxicity from free

ionic zinc, with nominal concentrations ranging from $ZnCl_2$ 0.136 to 1360 mg/L. Animal survival was checked at the beginning of each day, and the LC_{50} (96 h) for both compounds were estimated based on PROBIT analysis (Finney, 1978).

A second experiment was carried out based on the LC_{50} (96 h) determination for *C. gigas*. Animals were exposed to 4 mg/L ZnONP (approximately 1/10 of the LC_{50}) for 6, 24 or 48 h. The water was changed after 24 h, with ZnONP renewal. After exposure, gills and digestive gland were dissected for chemical and TEM analyses. This experiment had only one control group, which was sampled at the end of the exposure (48 h) along with all other groups. Aliquots of seawater were collected at 6, 24 and 48 h after exposure for chemical analysis. ZnONP was also added to additional aerated tanks without animals and aliquots were collected during the exposure period, in order to evaluate possible precipitation of ZnONP over the exposure time.

In a third experiment, animals were exposed only to ZnONP 4 mg/L for 24 or 48 h. The water was changed after 24 h, with ZnONP renewal. After exposure, hemolymph, gills and digestive gland were collected for cellular and biochemical analyses. A control group was used for each exposure period (24 and 48 h).

Due to the low solubility of butyl acetate in seawater, for all experiments ZnONP dispersion was firstly solubilized with DMSO. For the animal survival experiment, the butyl acetate (Sigma Aldrich) and DMSO (Sigma Aldrich) concentration in seawater of all groups (including control groups) was adjusted to the final level of 80 and 102 µg/L, respectively (values related to ZnONP 50 mg/L, highest concentration). For the other experiments, the levels of butyl acetate and DMSO were adjusted to 6.4 and 102 µg/L, respectively, (values related to ZnONP 4mg/L) for all groups analyzed (including controls). These values are at least 15,000 times below the LC_{50} (96 h) for other aquatic species (fish and invertebrates), according to the manufacturer's toxicological information. During exposure animals were not fed and were maintained in glass aquaria, which were cleaned every day with 5% HNO_3, on the moment of water change. The seawater pH was checked daily with pH strips for all groups, ranging from 7.5 to 8.0 and seawater salinity of 35‰.

2.3. Total zinc and ionic zinc determination

Chemical analyses were carried out in seawater and in tissues after exposure, according to a standardized protocol used earlier by our group with the blue mussel *Mytilus edulis* (Trevisan et al., 2011). To analyze the ionic zinc levels released by ZnONP dissociation, seawater samples were filtered using centrifugal filtering devices of regenerated cellulose with 10 KDa cutoff (Millipore), corresponding to the removal of nanoparticles with diameter higher than 2 nm. Prior analysis, all seawater samples (3 replicates per exposure time) were acidified to 5% HNO_3, while 500 mg of dried

tissue (4 replicates per group, each replicate consisted of a pool of two animals) were digested with 7 ml of concentrated HNO_3 and HCl (1.5:1 vol:vol) in a hot plate, and diluted to 50 ml with ultrapure water. Samples were analyzed for total zinc content by inductively coupled plasma optical - emission spectrometer (ICP-OES).

2.4. TEM analysis

TEM analyses were carried out on tissues after all exposure periods. For observation under the transmission electron microscope, samples approximately 5 mm length samples were obtained from both tissues: longitudinal sections from gills filaments near the external area and cross section of inner region of digestive gland. Samples were fixed overnight with 2.5% glutaraldehyde in 0.1 M sodium cacodylate buffer (pH 7.2), 0.2 M sucrose (Schmidt et al., 2009). The material was post-fixed with 1% osmium tetroxide for 4 h, dehydrated in an acetone gradient series, and embedded in Spurr's resin. Thin sections were stained with aqueous uranyl acetate followed by lead citrate. Four replicates were made for each experimental group; two samples per replication were then examined under TEM with a JEM 1011 at 80 kV. The cells analyzed by TEM were ciliated and microvilli epithelial cells from gill filaments and digestive cells from digestive tubules for the digestive gland. Similarities based on the comparison of individual treatments with replicates suggested that the ultrastructural analyses were reliable. Representative images of the cells identified and analyzed can also be visualized in the Supplementary Figure 1.

2.5. Biochemical analysis

Gills and digestive glands were collected from animals previously exposed to ZnONP for 24 and 48 h and their respective control groups (7 animals per group).

For total glutathione (GSH-t) and total protein (PSH) analyses, tissues (50 mg wet tissue) were freshly homogenized (1:10 vol:vol) in 0.5 M perchloric acid (PCA) and centrifuged at 15,000 x g for 2 minutes at 4˚C. The supernatant was used for total glutathione (GSH-t) while the pellet was used for total protein thiol (PSH) levels. For the determination of oxidized glutathione (GSSG), tissues (100 mg wet tissue) were freshly homogenized in 0.1 M potassium phosphate buffer, 1 mM ethylenediaminetetraacetic acid, pH 7.0, containing 10 mM N-ethylmaleimide to avoid further artfactual glutathione oxidation. Samples were acidified to 0.5 M PCA, centrifuged at 15,000 x g for 2 minutes at 4˚C and the pellet was discarded. N-ethylmaleimide removal was achieved using an alkaline hydrolysis procedure (Sacchetta et al., 1986). GSH-t and GSSG levels were determined by a coupled enzymatic assay at 340 nm (Akerboom and Sies, 1981), while PSH levels were determined by a colorimetric assay at 412 nm (Jocelyn, 1987).

For determination of glutathione reductase (GR), thioredoxin reductase (TrxR) and glutathione peroxidase (GPx) activity 400 mg of tissue was homogenized (1:4 vol:vol) in 20 mM (4-(2-hydroxyethyl)-1-piperazineethanesulfonic acid) pH 7.0 buffer and centrifuged at 20,000 x g for 30 minutes at 4 ˚C. The supernatant, which contains cytosolic proteins, was stored at -80˚C. For catalase (Cat) activity determination, 50 mg of tissue were homogenized using the same buffer but centrifuged at 1,000 x g for 10 min followed by 2,000 x g for 10 min for removal of nuclei and debris and the supernatant, which also contains the peroxisomes, was stored at -80˚C. Standardized spectrophotometric methods were used for determination of GR (Carlberg and Mannervik, 1985), TrxR (Arnér et al., 1999), GPx (Wendel, 1981), and Cat (Aebi, 1984).

For estimation of lipid peroxidation, 20 mg of tissue was homogenized (1:4 vol:vol) in 1.15% KCl containing 35 µM butylated hydroxytoluene and assayed colorimetrically at 532 nm for thiobarbituric acid reactive species (TBARS) according to a standard protocol (Oakes and Van Der Kraak, 2003).

Protein determination was carried out with the Bradford assay (Bradford, 1976) with bovine serum albumin as standard.

2.6. Immunological analysis

Hemocytes were collected from the adductor muscle of animals exposed to ZnONP 4 mg/L for 48 h, in a total of 7 pools of 2 animals per group, and kept on ice until analysis. Total hemocyte counting (THC) was assayed by optical microscopy using an improved Newbauer chamber. Cellular viability and immunological function assays were carried out according to previously-published procedures of our group (Mello et al., 2012, 2013; Trevisan et al., 2012).

Briefly, for the dimethyl thiazolyl diphenyl tetrazolium salt (MTT) assay, $0.4 \cdot 10^6$ cells were incubated with MTT 0.5 mg/L for 1 h and assayed at 550 nm while, for the neutral red assay (NR), 10^6 cells were incubated in neutral red 0.004% for 3 hours and assayed at 560 nm in an Infinite 200 PRO plate reader (Tecan, Brazil). Hemocyte phagocytosis was assessed using fluorescent beads (2.5%, Polysciences Inc., Paris, France), and defined as the percentage of cells able to ingest 3 or more beads. Intracellular ROS production was analyzed using 50 µM dichlorofluorescin diacetate (DCFDA). Both these later methods were assayed by flow cytometry using a FACSCanto II (BD Biosciences, Brazil).

2.7. Statistical analysis

For the survival experiment, the LC_{50} (96 h) was calculated based on the PROBIT values. Results were checked for normality distribution by Shapiro-Wilk normality test. Differences in variances and multiple comparisons were made by one-way Analysis of Variance followed by the

Duncan *post hoc* test when appropriate or by Student's t-test to compare two groups. Data are presented as mean ± SD.

3. Results

3.1. ZnONP characterization

ZnONP were characterized by three different methods: TEM, DLS and UV-VIS spectroscopy. TEM images indicate that ZnONP in seawater presented a round shape and an average primary nanoparticle size of 31.7 ± 13.0 nm (Fig. 1A), although aggregation behavior was observed (Fig. 1E). The UV-VIS absorption spectrum of ZnONP showed a high absorbance over the entire UV region presenting a small peak at 375 nm (Fig. 1B), just as expected for this nanomaterial. DLS analysis indicated different patterns for ZnONP dispersion according to the media used: in pure DMSO (Fig. 1C) particles size remained at the nanometer scale, with an average diameter of 28.6, 29.9 and 88.5 nm for the tested concentrations (8, 16 and 32 mg/L). However, in seawater (Fig. 1D) the average diameter increased to the micrometer range (1.02 µm and 2.05 µm for 8 and 16 mg/L, respectively). High aggregation behavior was detected in 32 mg/L ZnONP seawater samples preventing an accurate DLS analysis.

3.2. Acute toxicity test

The acute toxicity of ZnONP to the oyster, *C. gigas,* was evaluated by a survival experiment (Supplementary Figure 2). Although it was not possible to achieve 100% mortality with the highest concentrations (50 mg/L), it was possible to estimate the LC_{50} (96 h) to be 37.2 mg/L (corresponding to 29.9 mg/L of zinc). Soluble zinc ($ZnCl_2$) presented a similar toxicity with a LC_{50} (96 h) of 55.5 mg/L (corresponding to 26.6 mg/L of zinc) (Supplementary Figure 2).

3.3. Chemical analysis

Based on the survival experiments, oysters were exposed to a sub-lethal ZnONP concentration of 4 mg/L (approximately 10% of the LC_{50}). The total zinc content was analyzed in seawater, gills and digestive gland by ICP-OES at 6, 24 and 48 h post exposure.

For a 4 mg/L ZnONP solution, the levels of total zinc are expected to be approximately 3.2 mg/L. After ZnONP addition, the average total zinc content in the seawater, at time zero, was between 2.4 – 2.9 mg/L, which are 10 – 25% lower than the expected values, but considered acceptable for the purpose of this study (Fig. 2A). The levels of total zinc decreased 25 – 35% within 24 h in tanks

containing or lacking animals (Fig. 2A). A fine “dust” layer could be observed at the bottom surface of aquaria, indicating ZnONP precipitation over the time probably because of aggregation.

It was also assessed if ZnONP can release ionic zinc in seawater during 24 h (Fig. 2B). Using ultrafiltration with 10 KDa cutoff, what excludes ZnONP with diameter higher than 2 nm, soluble zinc was estimated. At time 0 h, just after the addition of ZnONP to seawater, the levels ionic zinc already corresponded to 38%, and increased overtime to 51 and 78% after 6 and 24 hours. This indicates a very fast initial dissociation of zinc from the ZnONP particle, within minutes, followed by a more slow release (hours).

The levels of total zinc in gills and digestive gland of oyster were also evaluated after 6, 24 and 48 h (Fig. 2C). The basal zinc concentration was approximately 2 times higher in gill (0.55 mg/kg) as compared to digestive gland (0.28 mg/kg). It was possible to track the accumulation of zinc in both tissues. Gills presented a 49 and 80% increase in zinc levels after 24 and 48 h, respectively, while zinc in digestive gland increased (+134%), but only after 48 h post exposure (Fig. 2C).

3.4. TEM analysis

When observed by TEM the cytoplasm of ciliated and microvilli epithelial cells from gill filaments of control animals (Fig. 3A and B) showed typical morphology, with intact nucleus (Fig. 3A, arrows) and mitochondrial cristae (Fig. 3B, arrows). In as little as 6 h of exposure to ZnONP (Fig. 3C-D) the mitochondria showed loss of mitochondrial cristae (Fig. 3C) and a number of endocytic vesicles were evident (Fig. 3C-D, arrows) in the cytoplasm near the cell membrane, which were absent in cells from control animals. Electron-dense particles were detected inside these vesicles, suggesting possible uptake of ZnONP by endocytosis, which remains to be confirmed. Damage to cell structures increased after 24 h of exposure (Fig. 3E-F), such as swollen mitochondria and a more conspicuous loss of mitochondrial cristae (Fig. 3E). After 48 h of exposure (Fig. 3G-H) the cytoplasmic space presented numerous vesiculated particles (Fig. 3G, arrows) and mitochondria with disrupted membranes (Fig. 3I). The general picture indicates that cell condition deteriorated with increasing time.

For digestive gland, the cytoplasm of digestive cells of control *C. gigas* (Fig. 4A-B) showed a nucleus with marginal chromatin (Fig. 4A), normal rough endoplasmic reticulum (Fig. 4A, arrows indicating the ribosomes) and intact mitochondrial cristae (Fig. 4B, arrows). After 6 h of ZnONP exposure (Fig. 4C-E), the cytoplasm still presented intact nucleus and rough endoplasmic reticulum (Fig. 4C), a large quantity of vesicles (Fig. 4C), and mitochondria with intact mitochondrial cristae (Fig. 4D and E, arrows). After 24 h (Fig. 4F-H) and 48 h (Fig. 4I and J), similarly to gills, it was observed mitochondrial cristae disruption (Fig. 4F, G and J) and the cytoplasm became highly vesiculated (Fig.

4H and I). Again, it was possible to detect highly electron-dense particles inside vesicles at 24 and 48 h (Fig 4H and I, arrows), but not at 6 h of exposure.

3.5. Biochemical analysis

Thiol levels were analyzed in gill and digestive gland of oysters after 24 or 48 h of exposure. In gill, no alterations were observed in GSH-t levels (Fig. 5A), GSSG (Fig. 5B) or GSH/GSSG ratio (not shown), but a 21% decrease in PSH levels was evident in gill of animals exposed for 48 h to ZnONP (Fig. 5C). Unexpectedly, a 62% increase in PSH levels was also detected in control animals after 48 h compared to control animals after 24 h (Fig. 5C). No differences were detected in GSH-t (Fig. 5A), GSSG (Fig. 5B) and PSH (Fig. 5C) levels or GSH/GSSG ratio (not shown) in the digestive gland of exposed animals, as compared to control animals.

A decrease of GR activity was detected in gill after 24 (–29%) and 48 h (–28%) of exposure, when compared to control animals, while this decrease (–47%) only occurred after 48 h of exposure in digestive gland (Fig. 6A). On the other hand, GPx activity (Fig. 6C) was 27% higher in gills after 48 h of exposure, respectively, but remained unchanged in digestive gland. For TrxR (Fig. 6B) and Cat (Fig. 6D) no significant alterations were detected after ZnONP exposure. Signals of oxidative damage were identified in gills of exposed oysters as a 49% increase in TBARS levels after 48 h of exposure, when compared to control group (Fig. 6E). Control animals after 48 h presented 38% decrease in TBARS levels when compared to control animals after 24 h (Fig. 6E).

3.6. Immunological parameters

After 48 h of exposure hemocytes were collected and assayed for cellular and immunological functions (Supplementary Figure 3). ZnONP caused no alterations on total hemocyte count or cellular viability (MTT and neutral red assay). Analysis of ROS production and phagocytosis by flow cytometry were also performed with hemocytes, but no significant alterations were detected.

4. Discussion

Pacific oysters, *C. gigas*, were exposed to ZnONP and animal survival, chemical, biochemical and cellular analyses were performed in order to understand the fate and effects initially characterize ZnONP toxicity.

The predicted environmental concentrations of ZnONP (most frequent value) for U.S. and Europe can range from 1-10 ng/L for natural surface water and 300-432 ng/L for effluents from sewage

treatment plants (Gottschalk et al., 2009). For soluble zinc, concentrations are usually at the nanomolar levels, but can reach micromolar levels in polluted areas (García et al. 2008; Srinivasa et al. 2008; Voets et al. 2009). Although the ZnONP concentration used in this study has probably not been reached in natural seawater, it can help to identify toxic and lethal concentrations to oysters as well as to elucidate its mode of action (toxicity and fate). These are important information not presently available, since this is one of the first toxicological studies with ZnONP in marine bivalves.

Before animal exposure, ZnONP were characterized by TEM and UV-VIS spectroscopy to confirm their nano-scale size (Fig. 1). The majority of the ZnONP (more than 60%) had a primary particle size ranging from 20 to 40 nm, and less than 1% had particle size higher than 80 nm, but presenting aggregation behavior in seawater. This was confirmed by comparing the diameter size of the dispersion by DLS in DMSO or seawater, where the average particles size increased from ~30 nm in DMSO to 1 - 2 μm in seawater (8 and 16 mg/L ZnONP) (Fig. 1).

An initial acute toxicity test (96 h) with ZnONP and *C. gigas* estimated the LC_{50} (96 h) as approximately 37 mg/L, corresponding to 29.9 mg of zinc per litter (Supplementary Figure 2). Soluble zinc ($ZnCl_2$) presented a similar toxicity (Supplementary Figure 2). The actual acute toxicity data of ZnONP to invertebrate and vertebrate aquatic species indicate that, although variable, the values of LC_{50} (96 h) are usually at the low mg/L range: 0.85 mg/L for the copepod *Tigriopus japonicas* (Wong et al., 2010); 1.19 mg/L for the amphipod *Elasmopus rapax* (Wong et al., 2010); 3.97 mg/L for the fish *Dano rerio* (Yu et al., 2011); 42.67 mg/L for the gastropod *Lymnaea luteola* (Ali et al., 2012). Other studies failed to detect 50% mortality even with concentrations such as 50 and 100 mg/L for carps and shrimps, respectively (Ates et al., 2012; Hao and Chen, 2012), suggesting that ZnONP toxicity can be extremely variable depending their physical-chemical properties and on the species.

Few studies have been conducted with ZnONP toxicity in bivalves. Recently it has been indicated mussels can be extremely efficient in filtering out suspended ZnONP, with further excretion by pseudofeces but still accumulating a high fraction in soft tissue (Montes et al., 2012). Zinc accumulation, increased respiration rate, slowed shell growth rate and increased mortality were observed in mussels exposed to ZnONP, indicating high energy demand to cope with the excess of zinc uptake (Hanna et al., 2013). These data are corroborated by an increase in lipid peroxidation and metallothionein levels in freshwater mussels (Gagné et al., 2013) or behavioral disturbances and increased catalase activity in marine clams (Buffet et al., 2012). In contrast, soluble zinc toxicity to bivalves is well documented, with accumulation occurring mainly in epithelial tissues (George and Pirie et al., 1980) impaired development (Fathallah et al., 2010) and physiology (Hietanen et al., 1988), oxidative and cellular stress (Devos et al., 2012; Franco et al., 2006; Trevisan et al., 2013) and immunologic disturbance (Taylor et al., 2013).

To elucidate how ZnONP causes toxicity to *C. gigas*, animals were exposed to a sub-lethal concentration of ZnONP (4 mg/L) for 6, 24 or 48 h. Without the ability to cross biological membranes and the absence of known transporters, nanoparticles must be taken up by cellular processes such as endocytosis (Moore, 2006). The presence of highly electron-dense particles inside vesicles in both tissues was observed only in animals exposed to ZnONP (Fig. 3 and 4), which corroborates the idea of intracellular uptake by endocytosis, although it cannot be a conclusive finding. ZnONP toxicity could also be related to the high dissociation rate of ZnONP in seawater (Fig. 2B) and therefore uptake of soluble zinc. In order to investigate this hypothesis oysters were exposed to ionic zinc ($ZnCl_2$) and the LC_{50} (96 h) of $ZnCl_2$ and ZnONP were compared (Supplementary Figure 2B and D). Data demonstrated that both compounds present similar values, corresponding to 29.9 (ZnONP) and 26.6 ($ZnCl_2$) mg of zinc per litter for each compound. The data suggest that uptake of dissociated ionic zinc play an important role on the toxicity to *C. gigas*.

Chemical analysis of gills and digestive gland indicate that ZnONP are initially incorporated by gills, although are accumulated preferably at digestive gland at 96h (Fig. 2). Some studies suggest that the uptake of nanoparticle by bivalves can occur preferentially by digestive organs (Al-Subiai et al., 2012; García-Negrete et al., 2013; Joubert et al., 2013; Moore, 2006; Tedesco et al., 2010a), nevertheless it has been demonstrated that gills can also be a main target for nanoparticles (Koehler et al., 2008). These data indicate that rate of accumulation, routes of uptake and distribution of nanoparticles are essential factors to be investigated in order to characterize their toxicity in bivalves.

Tissues were analyzed by TEM to investigate the presence or absence of ZnONP inside cells. According to TEM images, highly electron-dense particles were detected inside endocytic vesicles (Fig. 3 and 4), but not free within the cytosol. This suggests that nanoparticles were taken up by endocytosis, but we cannot rule out the possibility of artefactually producing such electron-dense area inside vesicles. The cytosolic enzyme GR showed lower activity and mitochondria were disrupted by ZnONP exposure. Based on a previous study with mussels (Franco et al., 2006) showing that GR can be inhibited by soluble zinc and that mammalian mitochondria are major targets for free zinc toxicity (Bossy-Wetzel et al., 2004), the data suggest that zinc ions are reaching the cytoplasm and mitochondria by two possible processes: (i) dissolution of ZnONP inside acidic vesicles such as endosomes and lysosomes with further leakage to cytosol; or (ii) ZnONP dissolution on seawater during exposure (Fig. 2B), causing the uptake of zinc ions.

The alterations in mitochondrial cristae and mitochondrial disruption detected by TEM, after ZnONP exposure (Fig. 3 and 4), indicate an important role on mitochondrial damage. In mammalian skin cells and retinal ganglion cells, uptake of ZnONP caused an increase in ROS production, leading to mitochondrial dysfunction and cell death (Guo et al., 2013; Yu et al., 2013). The results of the present

study also agree with previous data on blue mussel hemocytes where ZnONP increased the production of extracellular ROS in parallel to a decrease in mitochondrial mass/number and membrane potential (Ciacci et al., 2012). Taken together, these data suggest that ZnONP toxicity may correlates with ROS production, oxidative stress and mitochondrial impairment in marine bivalves as well.

After the uptake of nanomaterials by tissues such as gill and digestive gland, these compounds can reach the hemolymph and then affect immunological cells. Different *in vitro* studies with hemocytes and nanoparticles have reported the loss of cellular viability, negative effects on phagocytic activity; increased production of intra or extracellular ROS and mitochondrial impairment (Canesi et al., 2008, 2010; Ciacci et al., 2012). Surprisingly, functional analyses of hemocytes indicated no *in vivo* effects of ZnONP on cellular density, viability, ROS production and phagocytic activity, indicating that the immune system of *C. gigas* is either not affected at 48h, the immunological events are occurring in a different time point or higher levels are required to affect the immunological function of this species.

At least two signs of oxidative stress could be detected in gills of *C. gigas* after ZnONP exposure: lower levels of PSH (Fig. 5D) and higher levels of TBARS (Fig. 6E), while no effects were observed in digestive gland. It is important to note that in the present study the PSH and TBARS absolute values for control groups were statistically different after 24 and 48 h, with an increase in PSH and decrease in TBARS levels after 48 h (Fig. 5D and 6E). Therefore, it cannot be excluded that this variability in control group may affect statistical results, making it difficult to interpret the effects of ZnONP on oxidative stress.

Protein thiols have been considered an important mechanism of cellular defenses contributing quantitatively to redox buffering. They are susceptible to oxidation by ROS and therefore to reversible or irreversible protein inactivation and loss of function (Kiley and Storz, 2004; Leichert et al., 2008; Reischl et al., 2007). Protein thiol oxidation analysis (by proteomic or colorimetric assays) have been used in marine bivalves as an important tool to detect the toxic effects of different chemicals such as nanoparticles, quinones, polyphenols and metals (Łabieniec and Gabryelak, 2006; McDonagh and Sheehan, 2008; Tedesco et al., 2010a, 2010b; Trevisan et al., 2011), indicating that oxidation of protein thiols can be used as a marker for toxicity of environmental pollutants. Lipid peroxidation processes are another common result of exposure to oxidant agents, causing cellular membrane disturbances that can lead to cell death (Girotti, 1998). Various studies have reported increase in lipid peroxidation processes in bivalves exposed to nanoparticles, both in gills and digestive gland (Gomes et al., 2012, 2011; Kádár et al., 2010), confirming the toxic and oxidative effect of nanomaterials to aquatic species.

Activities of four important antioxidant enzymes were also assessed to better characterize the antioxidant system. Decreased GR (Fig. 6A) was a major effect of ZnONP, occurring in both gills and digestive gland exactly at the same exposures periods with zinc accumulation (Fig. 2B): 24 and 48 h for

gills, 48 h for digestive gland. Inhibition of this ancillary enzyme by soluble zinc has previously been detected earlier by our group in different organisms, such as mussels (Franco et al., 2006), fish (Franco et al., 2008a) and rats (Franco et al., 2008b; Maris et al., 2010), suggesting a key role for this enzyme in the mechanism of zinc toxicity. Alterations in GR activity can cause a disturbance on the reduction of GSSG under oxidative conditions, increasing the susceptibility of the organism to oxidative damage (Mitozo et al., 2011), however our data showed that GSSG or GSH were not altered by ZnONP exposure.

Despite the increased lipid peroxidation, protein thiol oxidation and GR inhibition in gills, as well as mitochondrial damage in gills and digestive gland, no effects were observed in other classical antioxidant-related parameters after ZnONP exposure, such as GSH-t (Fig. 5A) and GSSG (Fig. 5B) levels, GSH/GSSG ratio (data not shown) and other antioxidant enzymes activities (thioredoxin reductase and catalase, Fig. 6). In addition, hemocyte cellular function and viability were not affected as well (Supplementary Figure 3), rejecting the idea of a more broad effect on different tissues and organs. These data suggest that although there are signals of a pro-oxidant scenario and oxidative damage, especially in gills, ZnONP is not able to cause an intense or severe oxidative stress using this exposure protocol and time points in *C. gigas*.

Increased GPx activity was detected in gills after 48 h of exposure (Fig. 6C) could be an adaptive response to this mild pro-oxidant scenario. Increased GPx has previously been reported in gills of *C. gigas* and mussels *Perna perna* exposed to zinc (Cong et al., 2012; Franco et al., 2006). Up-regulation of the antioxidant system can be achieved by the Nrf2-dependent pathway, which is sensitive to oxidants and electrophiles (Itoh et al., 2004). It is possible that the pro-oxidative condition caused by ZnONP exposure in *C. gigas* could trigger the Nrf2 pathway, leading to an adaptive response of the cell, as suggested in other studies with nanoparticles (Kang et al., 2012; Piret et al., 2012). Although no specific study about the Nrf2 pathway has been conducted in bivalves, we have previously detected a strong response of *C. gigas* exposed to the electrophile 1-chloro-2,4-dinitrobenzene, with increased GST activity and GSH synthesis (Trevisan et al., 2012), suggesting that this pathway could be activated during stressful situation in bivalves as well.

5. Conclusions

This study reports for the first time the *in vivo* toxicity of ZnONP to *C. gigas* oysters, where zinc accumulation was detected first in gills (24 h) and later in digestive gland (48 h). This accumulation can be related to uptake of nanoparticulated or soluble zinc, as high dissociation of ZnONP was detected,

releasing ionic zinc to seawater. TEM images revealed a possible uptake of ZnONP by endocytosis, together with time-dependent progression of mitochondrial impairment in gill and digestive gland. Immunological functions of hemocytes were not affected by ZnONP. Decreased GR activity was a clear effect of ZnONP exposure in both tissues, and may be an important toxicity factor. The pro-oxidant action of ZnONP was indicated by the oxidation of protein thiols and increased lipid peroxidation in gills, but not in digestive gland, which may suggest a delayed toxicity in the latter tissue. Overall, our study showed more rapid zinc incorporation in gills, as compared to digestive gland, and progressive mitochondrial damage that matched the time course of zinc absorption in both tissues, which caused a decrease in GR activity, induction of lipid peroxidation and loss of protein thiols in gills.

Disclosure/Competing Interest Declaration: All the authors declare to have no actual or potential conflict of interest including any financial, personal or other relationships with other people or organizations. The work described has not been published previously (except in the form of an abstract); it is not under consideration for publication elsewhere; and its publication is approved by all authors and tacitly or explicitly by the responsible authorities where the work was carried out, and if accepted, it will not be published elsewhere in the same form, in English or in any other language, without the written consent of the copyright holder. All the authors declare to have participated in this study, with the following participation: experimental design, Rafael Trevisan, Alcir L. Dafre and David Sheehan; methodological protocols, Rafael Trevisan, Alcir Luiz Dafre, Danielle F. Mello and David Sheehan; experiment assays, analysis, and article preparation, all authors.

Policy and ethics: This work has been carried out in accordance with *The Code of Ethics of the World Medical Association (Declaration of Helsinki) for animal experiments*.

ACKNOWLEDGMENTS

This work was supported by CNPq (National Council for Research Development), INCT-TA (National Institue of Science and Technology – Aquatic Toxicology) and FAPESC (Foundation for the Support of

Scientific and Technological Research in the State of Santa Catarina). The provided scholarships are sincerely appreciated: R.T. (CAPES); G.D. (CAPES); D.F.M. (CAPES); M.A. (PIBIC/CNPq/UFSC); E.C.S. (Postdoctoral Research of Post-Graduate Program in Cell Biology and Development,). A.L.D. and Z.L.B. are research fellows of CNPq. The authors would like to acknowledge the service provided by the Central Laboratory of Electron Microscopy (LCME) from Federal University of Santa Catarina - Brazil.

REFERENCES

Aebi, H., 1984. Catalase in vitro. Methods Enzymol. 105, 121–126.

Akerboom, T.P., Sies, H., 1981. Assay of glutathione, glutathione disulfide, and glutathione mixed disulfides in biological samples. Methods Enzymol. 77, 373–382.

Al-Subiai, S.N., Arlt, V.M., Frickers, P.E., Readman, J.W., Stolpe, B., Lead, J.R., Moody, A.J., Jha, A.N., 2012. Merging nano-genotoxicology with eco-genotoxicology: an integrated approach to determine interactive genotoxic and sub-lethal toxic effects of C(60) fullerenes and fluoranthene in marine mussels, Mytilus sp. Mutat. Res. 745, 92–103.

Ali, D., Alarifi, S., Kumar, S., Ahamed, M., Siddiqui, M.A., 2012. Oxidative stress and genotoxic effect of zinc oxide nanoparticles in freshwater snail Lymnaea luteola L. Aquat. Toxicol. 124-125, 83–90.

Arnér, E.S., Zhong, L., Holmgren, A., 1999. Preparation and assay of mammalian thioredoxin and thioredoxin reductase. Methods Enzymol. 300, 226–239.

Arora, S., Rajwade, J.M., Paknikar, K.M., 2012. Nanotoxicology and in vitro studies: the need of the hour. Toxicol. Appl. Pharmacol. 258, 151–165.

Ates, M., Daniels, J., Arslan, Z., Farah, I.O., Rivera, H.F., 2012. Comparative evaluation of impact of Zn and ZnO nanoparticles on brine shrimp (Artemia salina) larvae: effects of particle size and solubility on toxicity. Environ. Sci. Process. Impacts 15, 225–233.

Bossy-Wetzel, E., Talantova, M.V., Lee, W.D., Schölzke, M.N., Harrop, A., Mathews, E., Götz, T., Han, J., Ellisman, M.H., Perkins, G.A., Lipton, S.A., 2004. Crosstalk between nitric oxide and zinc pathways to neuronal cell death involving mitochondrial dysfunction and p38-activated K+ channels. Neuron 41, 351–365.

Bradford, M.M., 1976. A rapid and sensitive method for the quantitation of microgram quantities of protein utilizing the principle of protein-dye binding. Anal. Biochem. 72, 248–254.

Buffet, P.E., Tankoua, O.F., Pan, J.F., Berhanu, D., Herrenknecht, C., Poirier, L., Amiard-Triquet, C., Amiard, J.C., Bérard, J.B., Risso, C., Guibbolini, M., Roméo, M., Reip, P., Valsami-Jones, E., Mouneyrac, C., 2011. Behavioural and biochemical responses of two marine invertebrates Scrobicularia plana and Hediste diversicolor to copper oxide nanoparticles. Chemosphere 84, 166–174.

Buffet, P.E., Amiard-Triquet, C., Dybowska, A., Risso-de Faverney, C., Guibbolini, M., Valsami-Jones, E., Mouneyrac, C., 2012. Fate of isotopically labelled zinc oxide nanoparticles in sediment and effects on two endobenthic species, the clam Scrobicularia plana and the ragworm Hediste diversicolor. Ecotoxicol. Environ. Saf. 84, 191-198.

Canesi, L., Ciacci, C., Betti, M., Fabbri, R., Canonico, B., Fantinati, A., Marcomini, A., Pojana, G., 2008. Immunotoxicity of carbon black nanoparticles to blue mussel hemocytes. Environ. Int. 34, 1114–1119.

Canesi, L., Ciacci, C., Fabbri, R., Marcomini, A., Pojana, G., Gallo, G., 2012. Bivalve molluscs as a unique target group for nanoparticle toxicity. Mar. Environ. Res. 76, 16–21.

Canesi, L., Ciacci, C., Vallotto, D., Gallo, G., Marcomini, A., Pojana, G., 2010. In vitro effects of suspensions of selected nanoparticles (C60 fullerene, TiO2, SiO2) on Mytilus hemocytes. Aquat. Toxicol. 96, 151–158.

Carlberg, I., Mannervik, B., 1985. Glutathione reductase. Methods Enzymol. 113, 484–490.

Ciacci, C., Canonico, B., Bilaniĉovă, D., Fabbri, R., Cortese, K., Gallo, G., Marcomini, A., Pojana, G., Canesi, L., 2012. Immunomodulation by different types of N-oxides in the hemocytes of the marine bivalve Mytilus galloprovincialis. Plos One 7, e36937.

Cong, M., Wu, H., Liu, X., Zhao, J., Wang, X., Lv, J., Hou, L., 2012. Effects of heavy metals on the expression of a zinc-inducible metallothionein-III gene and antioxidant enzyme activities in Crassostrea gigas. Ecotoxicol. 21, 1928–1936.

Devos, A., Voiseux, C., Caplat, C., Fievet, B., 2012. Effect of chronic exposure to zinc in young spats of the Pacific oyster (Crassostrea gigas). Environ. Toxicol. Chem.31, 2841-2847.

Fathallah S, Medhioub MN, Medhioub A, Kraiem MM. Toxicity of Hg, Cu and Zn on early developmental stages of the European clam (Ruditapes decussatus) with potential application in marine water quality assessment. Environ. Monit. Assess. 171, 661-669.

Finney, D.J., 1978. Statistical Method in Biological Assay, third ed. Charles Griffin & Co., London.

Franco, J.L., Trivella, D.B.B., Trevisan, R., Dinslaken, D.F., Marques, M.R.F., Bainy, A.C.D., Dafre, A.L., 2006. Antioxidant status and stress proteins in the gills of the brown mussel Perna perna exposed to zinc. Chem. Biol. Interact. 160, 232–240.

Franco, J.L., Posser, T., Mattos, J.J., Sánchez-Chardi, A., Trevisan, R., Oliveira, C.S., Carvalho, P.S.M., Leal, R.B., Marques, M.R.F., Bainy, A.C.D., Dafre, A.L., 2008a. Biochemical alterations in juvenile carp (Cyprinus carpio) exposed to zinc: glutathione reductase as a target. Mar. Environ. Res. 66, 88–89.

Franco, J.L., Posser, T., Brocardo, P.S., Trevisan, R., Uliano-Silva, M., Gabilan, N.H., Santos, A.R.S., Leal, R.B., Rodrigues, A.L.S., Farina, M., Dafre, A.L., 2008b. Involvement of glutathione, ERK1/2 phosphorylation and BDNF expression in the antidepressant-like effect of zinc in rats. Behav. Brain Res. 188, 316–323.

Gagné, F., Turcotte, P., Gagnon, A.C., 2013. The effects of zinc oxide nanoparticles on the metallome in freshwater mussels. Comp. Biochem. Physiol. Toxicol. Pharmacol. 158, 22-28.

García-Negrete, C.A., Blasco, J., Volland, M., Rojas, T.C., Hampel, M., Lapresta-Fernández, A., Jiménez de Haro, M.C., Soto, M., Fernández, A., 2013. Behaviour of Au-citrate nanoparticles in seawater and accumulation in bivalves at environmentally relevant concentrations. Environ. Pollut. 1987 174, 134–141.

García, E.M., Cruz-Motta, J.J., Farina, O., Bastidas, C., 2008. Anthropogenic influences on heavy metals across marine habitats in the western coast of Venezuela. Cont. Shelf Res. 28, 2757-2766.

George, S.G., Pirie, B.J.S., 1980. Metabolism of zinc in the mussel, Mytilus edluis (L.): a combined ultraestructural and biochemical study. J. Mar. Biol. Assoc. UK 60, 575-590.

Girotti, A.W., 1998. Lipid hydroperoxide generation, turnover, and effector action in biological systems. J. Lipid Res. 39, 1529–1542.

Gomes, T., Pinheiro, J.P., Cancio, I., Pereira, C.G., Cardoso, C., Bebianno, M.J., 2011. Effects of copper nanoparticles exposure in the mussel Mytilus galloprovincialis. Environ. Sci. Technol. 45, 9356–9362.

Gomes, T., Pereira, C.G., Cardoso, C., Pinheiro, J.P., Cancio, I., Bebianno, M.J., 2012. Accumulation and toxicity of copper oxide nanoparticles in the digestive gland of Mytilus galloprovincialis. Aquat. Toxicol. 118-119, 72–79.

Gottschalk, F., Sonderer, T., Scholz, R.W., Nowack, B., 2009. Modeled environmental concentrations of engineeres nanomaterials (Tio2, Zno, Ag, CNT, fullerenes) for different regions. Environ. Sci. Technol. 43, 9216-9222.

Guo, D., Bi, H., Liu, B., Wu, Q., Wang, D., Cui, Y., 2013. Reactive oxygen species-induced cytotoxic effects of zinc oxide nanoparticles in rat retinal ganglion cells. Toxicol. In Vitro 27, 731–738.

Handy, R.D., Owen, R., Valsami-Jones, E., 2008. The ecotoxicology of nanoparticles and nanomaterials: current status, knowledge gaps, challenges, and future needs. Ecotoxicol. 17, 315–325.

Hanna, S.K., Miller, R.J., Muller, E.B., Nisbet, R.M., Lenihan, H.S., 2013. Impact of engineered zinc oxide nanoparticles on the individual performance of Mytilus galloprovincialis). PLoS ONE 8, e61800.

Hao, L., Chen, L., 2012. Oxidative stress responses in different organs of carp (Cyprinus carpio) with exposure to ZnO nanoparticles. Ecotoxicol. Environ. Saf. 80, 103–110.

Hietanen, B., Sunila, I., Kristoffersson, R., 1988. Toxic effect of zinc on the common mussel Mytilus edulis L. (Bivalvia) in brackish water. I. Physiological and histopathological studies. Ann. Zool. Fennici. 25, 341-347.

Hristozov, D.R., Gottardo, S., Critto, A., Marcomini, A., 2012. Risk assessment of engineered nanomaterials: a review of available data and approaches from a regulatory perspective. Nanotoxicol. 6, 880–898.

Itoh, K., Tong, K.I., Yamamoto, M., 2004. Molecular mechanism activating Nrf2-Keap1 pathway in regulation of adaptive response to electrophiles. Free Radic. Biol. Med. 36, 1208–1213.

Jocelyn, P.C., 1987. Spectrophotometric assay of thiols. Methods Enzymol. 143, 44–67.

Joubert, Y., Pan, J.F., Buffet, P.E., Pilet, P., Gilliland, D., Valsami-Jones, E., Mouneyrac, C., Amiard-Triquet, C., 2013. Subcellular localization of gold nanoparticles in the estuarine bivalve Scrobicularia plana after exposure through the water. Gold Bull. 46, 47–56.

Kádár, E., Lowe, D.M., Solé, M., Fisher, A.S., Jha, A.N., Readman, J.W., Hutchinson, T.H., 2010. Uptake and biological responses to nano-Fe versus soluble FeCl3 in excised mussel gills. Anal. Bioanal. Chem. 396, 657–666.

Kang, S.J., Ryoo, I.G., Lee, Y.J., Kwak, M.K., 2012. Role of the Nrf2-heme oxygenase-1 pathway in silver nanoparticle-mediated cytotoxicity. Toxicol. Appl. Pharmacol. 258, 89–98.

Kiley, P.J., Storz, G., 2004. Exploiting thiol modifications. Plos Biol. 2, e400.

Koehler, A., Marx, U., Broeg, K., Bahns, S., Bressling, J., 2008. Effects of nanoparticles in Mytilus edulis gills and hepatopancreas - a new threat to marine life? Mar. Environ. Res. 66, 12–14.

Łabieniec, M., Gabryelak, T., 2006. Oxidatively modified proteins and DNA in digestive gland cells of the fresh-water mussel Unio tumidus in the presence of tannic acid and its derivatives. Mutat. Res. 603, 48–55.

Leichert, L.I., Gehrke, F., Gudiseva, H.V., Blackwell, T., Ilbert, M., Walker, A.K., Strahler, J.R., Andrews, P.C., Jakob, U., 2008. Quantifying changes in the thiol redox proteome upon oxidative stress in vivo. Proc. Natl. Acad. Sci. U. S. A. 105, 8197–8202.

Ma, H., Williams, P.L., Diamond, S.A., 2013. Ecotoxicity of manufactured ZnO nanoparticles-a review. Environ. Pollut. 1987 172, 76–85.

Maris, A.F., Franco, J.L., Mitozo, P.A., Paviani, G., Borowski, C., Trevisan, R., Uliano-Silva, M., Farina, M., Dafre, A.L., 2010. Gender effects of acute malathion or zinc exposure on the antioxidant response of rat hippocampus and cerebral cortex. Basic Clin. Pharmacol. Toxicol. 107, 965–970.

McDonagh, B., Sheehan, D., 2008. Effects of oxidative stress on protein thiols and disulphides in Mytilus edulis revealed by proteomics: actin and protein disulphide isomerase are redox targets. Mar. Environ. Res. 66, 193–195.

Mello, D.F., de Oliveira, E.S., Vieira, R.C., Simoes, E., Trevisan, R., Dafre, A.L., Barracco, M.A., 2012. Cellular and transcriptional responses of Crassostrea gigas hemocytes exposed in vitro to brevetoxin (PbTx-2). Mar. Drugs 10, 583–597.

Mello, D.F., Silva, P.M. da, Barracco, M.A., Soudant, P., Hégaret, H., 2013. Effects of the dinoflagellate Alexandrium minutum and its toxin (saxitoxin) on the functional activity and gene expression of Crassostrea gigas hemocytes. Harmful Algae 26, 45–51.

Mitozo, P.A., de Souza, L.F., Loch-Neckel, G., Flesch, S., Maris, A.F., Figueiredo, C.P., Dos Santos, A.R.S., Farina, M., Dafre, A.L., 2011. A study of the relative importance of the peroxiredoxin-, catalase-, and glutathione-dependent systems in neural peroxide metabolism. Free Radic. Biol. Med. 51, 69–77.

Montes, M.O., Hanna, S.K., Lenihan, H.S., Keller, A.A., 2012. Uptake, accumulation, and biotransformation of metal oxide nanoparticles by a marine suspension-feeder. J. Hazard. Mater. 225-226, 139-145.

Moore, M.N., 2006. Do nanoparticles present ecotoxicological risks for the health of the aquatic environment? Environ. Int. 32, 967–976.

Nel, A., Xia, T., Mädler, L., Li, N., 2006. Toxic potential of materials at the nanolevel. Science 311, 622–627.

Oakes, K.D., Van Der Kraak, G.J., 2003. Utility of the TBARS assay in detecting oxidative stress in white sucker (Catostomus commersoni) populations exposed to pulp mill effluent. Aquat. Toxicol. 63, 447–463.

Piret, J.P., Jacques, D., Audinot, J.N., Mejia, J., Boilan, E., Noël, F., Fransolet, M., Demazy, C., Lucas, S., Saout, C., Toussaint, O., 2012. Copper(II) oxide nanoparticles penetrate into HepG2 cells, exert cytotoxicity via oxidative stress and induce pro-inflammatory response. Nanoscale 4, 7168–7184.

Reischl, E., Dafre, A.L., Franco, J.L., Wilhelm Filho, D., 2007. Distribution, adaptation and physiological meaning of thiols from vertebrate hemoglobins. Comp. Biochem. Physiol. Toxicol. Pharmacol. 146, 22–53.

Ringwood, A.H., McCarthy, M., Bates, T.C., Carroll, D.L., 2010. The effects of silver nanoparticles on oyster embryos. Mar. Environ. Res. 69 Suppl, S49–51.

Sacchetta, P., Di Cola, D., Federici, G., 1986. Alkaline hydrolysis of N-ethylmaleimide allows a rapid assay of glutathione disulfide in biological samples. Anal. Biochem. 154, 205–208.

Schmidt, E.C., Scariot, L.A., Rover, T., Bouzon, Z.L., 2009. Changes in ultrastructure and histochemistry of two red macroalgae strains of Kappaphycus alvarezii (Rhodophyta, Gigartinales), as a consequence of ultraviolet B radiation exposure. Micron 1993 40, 860–869.

Scown, T.M., van Aerle, R., Tyler, C.R., 2010. Review: Do engineered nanoparticles pose a significant threat to the aquatic environment? Crit. Rev. Toxicol. 40, 653–670.

Srinivasa, G.S., Govil, P.K., 2008. Distribution of heavy metals in surface water of Ranipet industrial area in Tamil Nadu, India. Environ. Monit. Assess. 136, 197-207.

Taylor, D.A., Thompson, E.L., Nair, S.V., Raftos, D.A., 2013. Differential effects of metal contamination on the transcript expression of immune- and stress-response genes in the Sydney Rock oyster, Saccostrea glomerata.Environ. Pollut. 178, 65-71.

Tedesco, S., Doyle, H., Blasco, J., Redmond, G., Sheehan, D., 2010a. Exposure of the blue mussel, Mytilus edulis, to gold nanoparticles and the pro-oxidant menadione. Comp. Biochem. Physiol. Toxicol. Pharmacol. 151, 167–174.

Tedesco, S., Doyle, H., Blasco, J., Redmond, G., Sheehan, D., 2010b. Oxidative stress and toxicity of gold nanoparticles in Mytilus edulis. Aquat. Toxicol. 100, 178–186.

Trevisan, R., Mello, D.F., Fisher, A.S., Schuwerack, P.-M., Dafre, A.L., Moody, A.J., 2011. Selenium in water enhances antioxidant defenses and protects against copper-induced DNA damage in the blue mussel Mytilus edulis. Aquat. Toxicol. 101, 64–71.

Trevisan, R., Arl, M., Sacchet, C.L., Engel, C.S., Danielli, N.M., Mello, D.F., Brocardo, C., Maris, A.F., Dafre, A.L., 2012. Antioxidant deficit in gills of Pacific oyster (Crassostrea gigas) exposed to chlorodinitrobenzene increases menadione toxicity. Aquat. Toxicol. 108, 85–93.

Trevisan, R., Flesch, S., Mattos, J.J., Milani, M.R., Bainy, A.C., Dafre, A.L., 2013. Zinc causes acute impairment of glutathione metabolism followed by coordinated antioxidant defenses amplification in gills of brown mussels *Perna perna*. Comp. Biochem. Physiol. Toxicol. Pharcol. 159, 22-30.

Voets, J., Redeker, E.S., Blust, R., Bervoets, L. 2009. Differences in metal sequestration between zebra mussels from clean and polluted field locations. Aquat. Toxicol. 93, 53-60.

Wendel, A., 1981. Glutathione peroxidase. Methods Enzymol. 77, 325–333.

Wong, S.W.Y., Leung, P.T.Y., Djurisić, A.B., Leung, K.M.Y., 2010. Toxicities of nano zinc oxide to five marine organisms: influences of aggregate size and ion solubility. Anal. Bioanal. Chem. 396, 609–618.

Yu, L., Fang, T., Xiong, D., Zhu, W., Sima, X., 2011. Comparative toxicity of nano-ZnO and bulk ZnO suspensions to zebrafish and the effects of sedimentation, ˙OH production and particle dissolution in distilled water. J. Environ. Monit. 13, 1975–1982.

Yu, K.-N., Yoon, T.J., Minai-Tehrani, A., Kim, J.E., Park, S.J., Jeong, M.S., Ha, S.W., Lee, J.K., Kim, J.S., Cho, M.-H., 2013. Zinc oxide nanoparticle induced autophagic cell death and mitochondrial damage via reactive oxygen species generation. Toxicol. in Vitro 27, 1187–1195.

Zak, A.K., Razali, R., Majid, W.H.A., Darroudi, M., 2011. Synthesis and characterization of a narrow size distribution of zinc oxide nanoparticles. Int. J. Nanomedicine 6, 1399–1403.

Zuykov, M., Pelletier, E., Belzile, C., Demers, S., 2011. Alteration of shell nacre micromorphology in blue mussel Mytilus edulis after exposure to free-ionic silver and silver nanoparticles. Chemosphere 84, 701–706.

FIGURE SUBTITLES

Fig. 1. Characterization of zinc oxide nanoparticles (ZnONP). (A) Primary particle size distribution was assessed by transmission electron microscopy (TEM) images of ZnONP in seawater; (B) Particle diameter evaluation by dynamic light scattering (DLS) analysis of 8-32 mg/L ZnONP samples in DMSO; (C) DLS analysis of 8 and 16 mg/L ZnONP samples in seawater (32 mg/L ZnONP was not possible to be analyzed due to high aggregation rate); (D) Representative TEM image of ZnONP in seawater highlighting the nanoparticle aggregation in the exposure media.

Fig. 2. Chemical analysis of seawater, gill and digestive gland of *Crassostrea gigas*. Animals were exposed to 4 mg/L of ZnONP and samples taken at indicated time points: (A) Levels of zinc in seawater in the presence (circles) or not (squares) of *C. gigas*. At 24 h, water was changed and ZnONP levels were renewed; (B) Solutions of 4 mg/L ZnONP in the absence of animals were analyzed for zinc ions release during 24 h after removal of nanoparticles by ultrafiltration; (C) Levels of zinc in gills and digestive gland of *C. gigas* during ZnONP exposure. Data are presented as mean ± SD, and analyzed by one-way analysis of variance followed by Duncan's *post hoc* test. Statistical differences between the groups for the same tissue are indicated as * ($p < 0.05$) or *** ($p < 0.001$).

Fig. 3. TEM micrographs of ciliated and microvilli epithelial cells of gills filaments from *Crassostrea gigas* exposed to 4 mg/L ZnONP. (A and B) cells of control animals showing normal morphology of mitochondria (M) and nucleus (N) with intact nuclear envelope (arrows); (B) detail of mitochondrial cristae (arrows); (C-D) cells after 6 h of exposure: absence mitochondrial cristae and presence of endocytic vesicles containing electron-dense particles (arrows); (E-F) cells after 24 h of exposure: (E) swollen mitochondria (arrows) and (F) intact nucleus; (G and H) cells after 48 h of exposure: (G) highly vesiculated cytoplasmic space (arrows) and (H) disrupted mitochondria.

Fig. 4. TEM micrographs of digestive cells from digestive tubules of *Crassostrea gigas* exposed to 4 mg/L ZnONP. (A and B) Control cells. Note normal morphology of nucleus (N) and rough endoplasmic reticulum (RER) with ribosomes attached (arrows) and (B) intact mitochondrial cristae (arrows); (C – E) cells after 6 h of exposure: (C) normal morphology of nucleus (N), rough endoplasmic reticulum, mitochondria (M) and vesicles (V), (D) detail of mitochondrial cristae (arrows) and (E) large quantity of lipid droplets (arrows); (F-H) cells after 24 h of exposure: (F and G) disrupted mitochondria and (H) large quantity of vesicles (V) in the cytoplasm with electron-dense particles (arrows); (I and J) cells after 48 h of exposure: (I) large quantity of vesicles (V) in the cytoplasm with electron-dense particles (arrows), and (J) changes in the mitochondria organization.

Fig. 5. Thiol status in gills and digestive gland of *Crassostrea gigas* exposed to 4 mg/L zinc oxide nanoparticles (ZnONP). (A) Levels of total glutathione (GSH-t); (B) Levels of oxidized glutathione (GSSG); (C) Levels of protein thiols (PSH); Data are presented as mean ± SD. Statistical analysis was independently analyzed by Student's t-test for each tissue and exposure period. Statistically significant differences between exposed and the respective control group are indicated as * ($p < 0.05$).

Fig. 6. Activity of antioxidant enzymes and lipid peroxidation index in gill and digestive gland of *Crassostrea gigas* exposed to 4 mg/L ZnONP. (A) Glutathione reductase (GR) activity; (B) Thioredoxin reductase (TrxR) activity; Glutathione peroxidase (GPx) activity; (D) Catalase (Cat) activity; Lipid peroxidation index measured by the TBARS. Data are presented as mean ± SD. Statistical analysis was independently analyzed by Student's t-test for each tissue and exposure period as well as to compare each control group (24 and 48h). Statistically significant differences are indicated as * ($p < 0.05$), ** ($p < 0.01$) and *** ($p < 0.001$).

Supplementary Figure 1. TEM representative micrographs of the analyzed cells in gill and digestive gland from oysters Crassostrea gigas. In gill, (A) the ciliated epithelial cel (CEC) containing cilia (Ci) and (B) microvilli epithelial cell (MEC) containing microvilli (Mi) are presented. In the digestive gland, it can be observed a basal region of the digestive acinum with stroma (S) and digestive cells (DC), containing many lipid droplets (LD).

Supplementary Figure 2. Acute toxicity test of ZnONP and $ZnCl_2$ in *Crassostrea gigas*. Animals were exposed to different concentrations of ZnONP (ranging from 0.05 to 50 mg/L) and $ZnCL_2$ (ranging from 0.136 to 1360 mg/L) for 96 h. The survival rate was assessed at the beginning of each day. Water was changed daily with concomitant ZnONP and $ZnCl_2$ levels renewal. (A) Graph representing the PROBIT analysis of the *C. gigas* survival rate during ZnONP exposure; (B) determination of the LC_{50} (96 h) for ZnONP based on the survival proportion of each group; (C) Graph representing the PROBIT analysis of the *C. gigas* survival rate during $ZnCl_2$ exposure; (D) determination of the LC_{50} (96 h) for $ZnCl_2$ based on the survival proportion of each group. In addition, the LC50 (96 h) of both compounds are presented as the corresponding levels of zinc in order to better compare the acute toxicity data of ZnONP and $ZnCl_2$.

Supplementary Figure 3. Hemocytes cellular and immunological analysis of *Crassostrea gigas* exposed to 4 mg/L ZnONP during 48 h. (A) Total hemocyte counting (THC); (B) Cellular viability measured by the MTT assay; (C) Cellular viability measured by the neutral red retention assay (NR); (D) Intracellular production of reactive oxygen species (ROS); (E) Percentage of phagocytic cells. Data are presented as mean ± SD. Statistical analysis was independently analyzed by Student's t-test for each tissue and exposure period. No statistically significant differences were detected between exposed and the respective control group are ($p > 0.05$).

Figure 1.

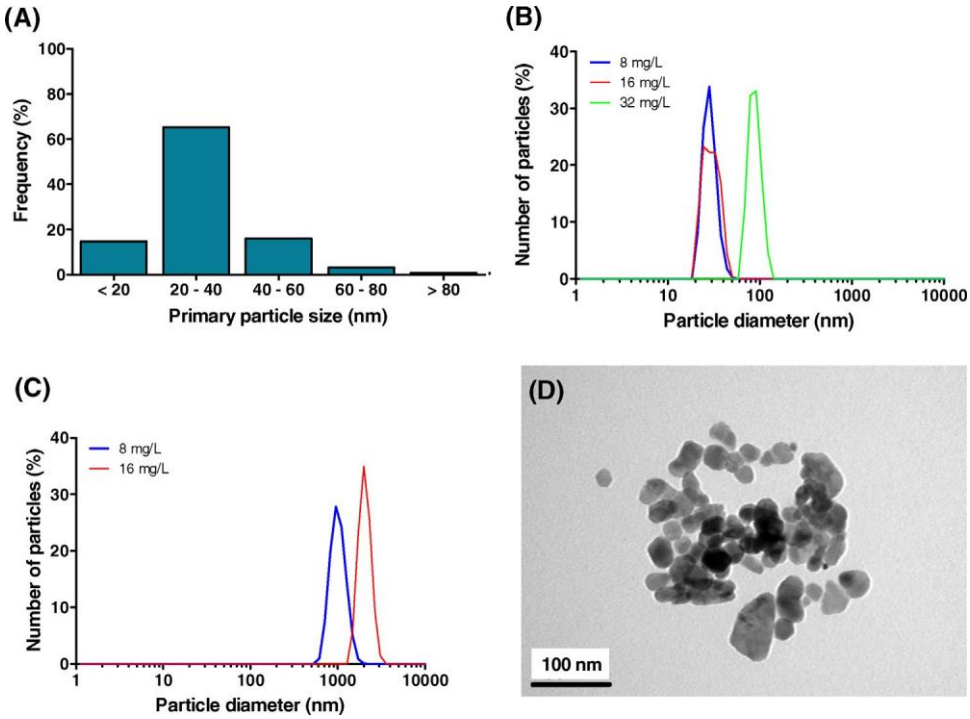

Figure 2.

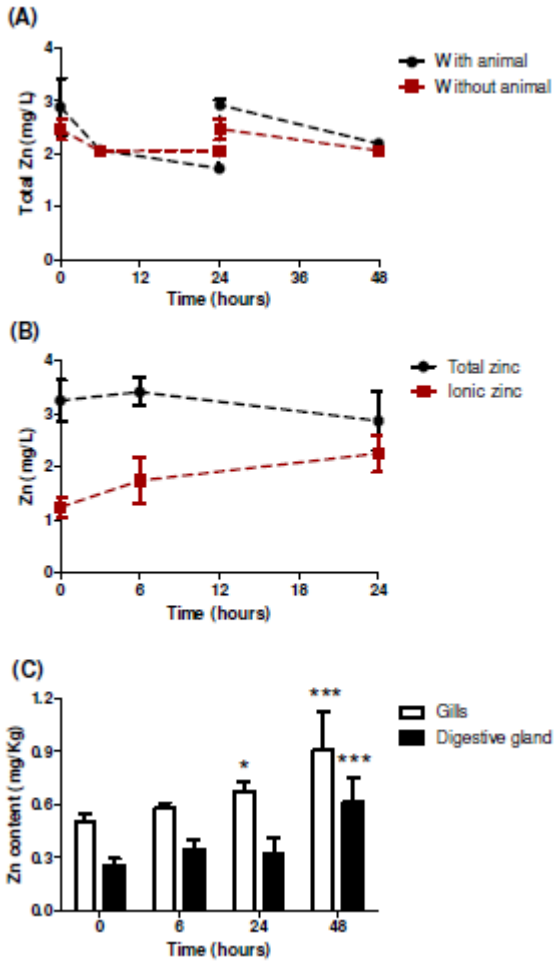

Figure 3.

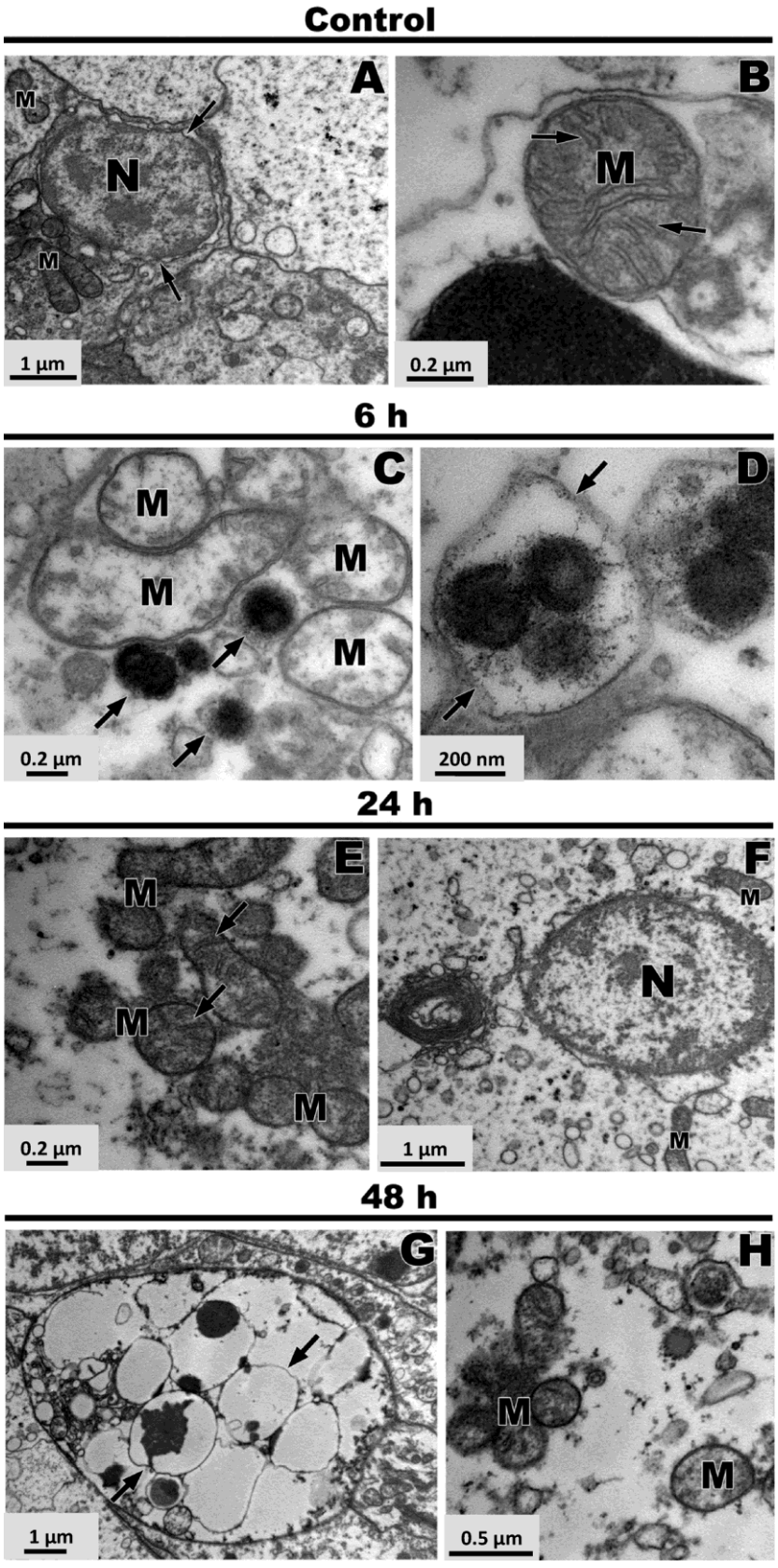
Control
A
M
N
M
1 µm
B
M
0.2 µm
6 h
C
M
M
M
M
0.2 µm
D
200 nm
24 h
E
M
M
M
0.2 µm
F
M
N
M
1 µm
48 h
G
1 µm
H
M
M
0.5 µm

Figure 4.

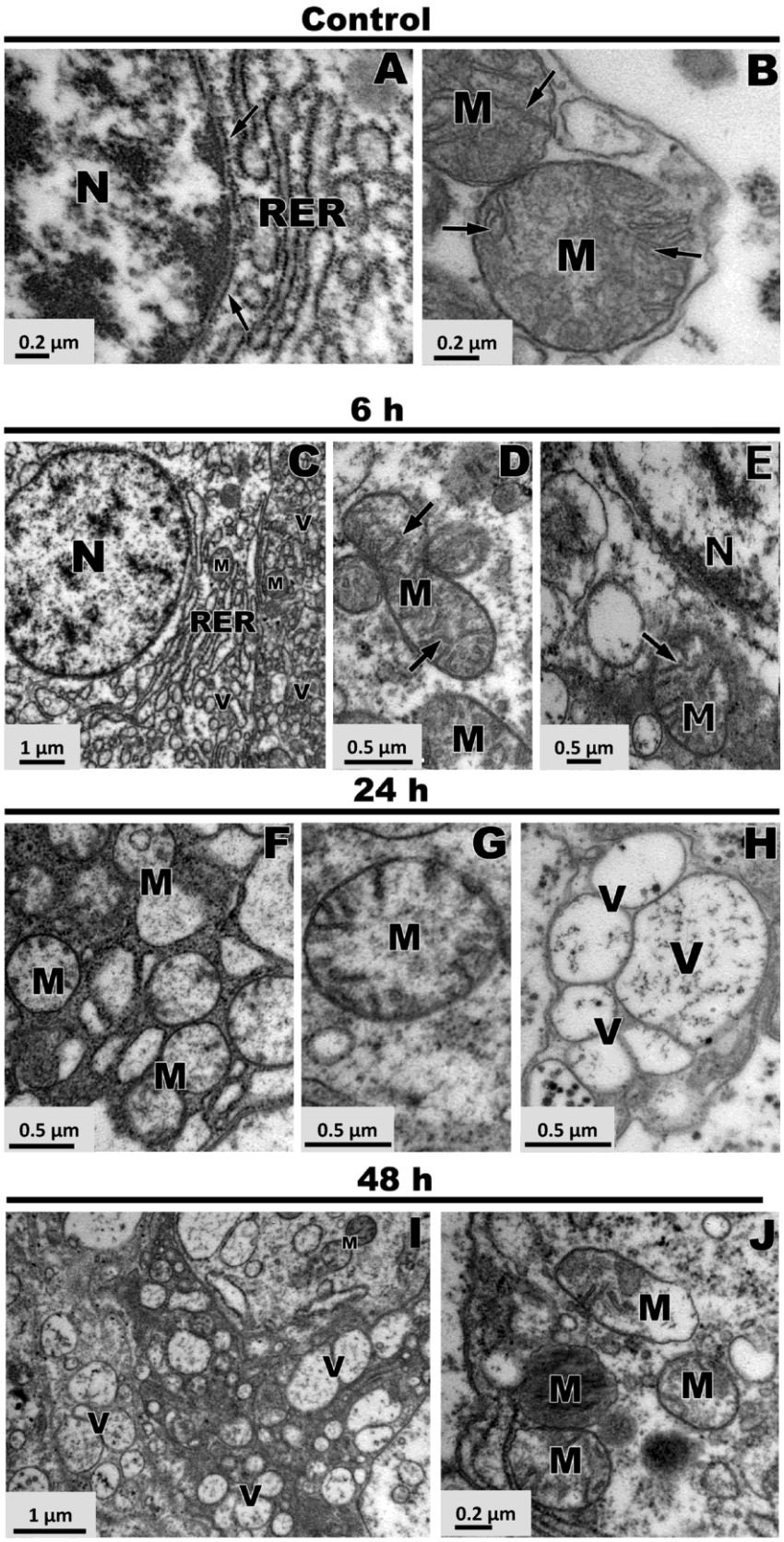
Control
A
N
RER
0.2 µm
B
M
M
0.2 µm
6 h
C
N
V
M
M
RER
V
V
1 µm
D
M
M
0.5 µm
E
N
M
0.5 µm
24 h
F
M
M
M
0.5 µm
G
M
0.5 µm
H
V
V
V
0.5 µm
48 h
I
M
V
V
V
1 µm
J
M
M
M
M
0.2 µm

Figure 5.

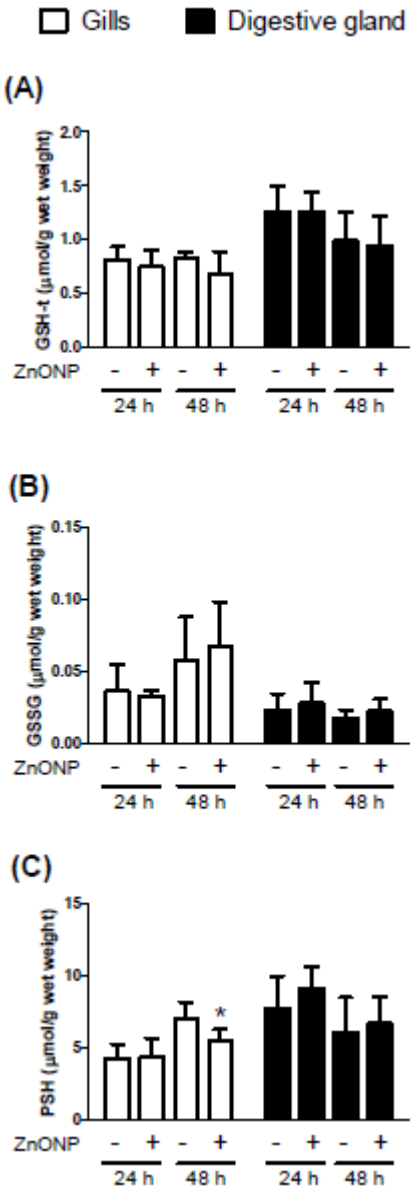
Gills
Digestive gland
(A)
GSH-t (µmol/g wet weight)
2.0
1.5
1.0
0.5
0.0
ZnONP - + - + - + - +
24 h
48 h
24 h
48 h
(B)
GSSG (µmol/g wet weight)
0.15
0.10
0.05
0.00
ZnONP - + - + - + - +
24 h
48 h
24 h
48 h
(C)
PSH (µmol/g wet weight)
15
10
5
0
*
ZnONP - + - + - + - +
24 h
48 h
24 h
48 h

Figure 6.

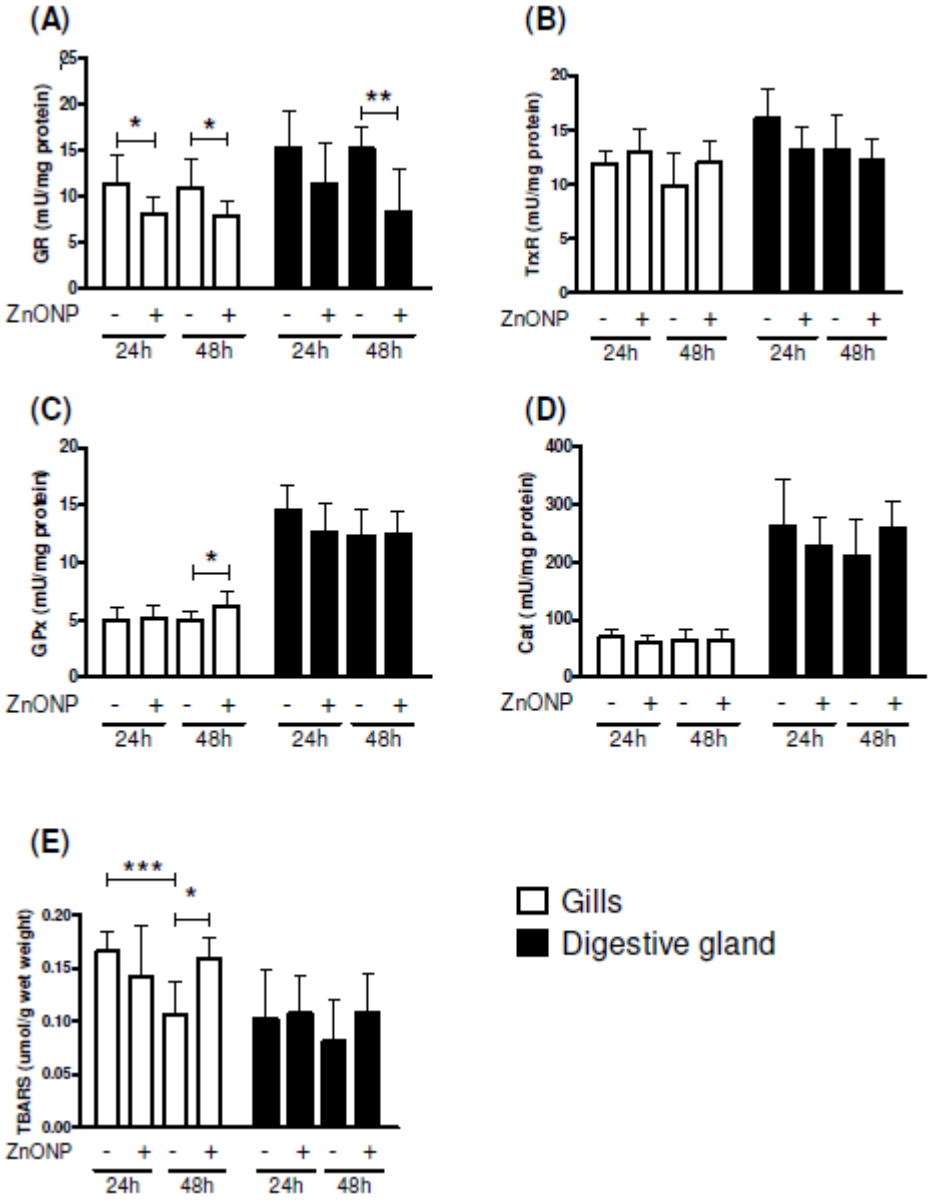
(A)
GR (mU/mg protein)
ZnONP
24h
48h
(B)
TrxR (mU/mg protein)
(C)
GPx (mU/mg protein)
(D)
Cat (mU/mg protein)
(E)
TBARS (umol/g wet weight)
Gills
Digestive gland